Short Communication

Preparation and Properties of Nano-multilayer Films by Rotating Jet Electrodeposition

Lida Shen[1,], Kailin Zhao[1], Mingbo Qiu, Xin Wang, Mingzhi Fan*

College of Mechanical and Electrical Engineering, Nanjing University of Aeronautics and Astronautics, No. 29 Yudao Street, Nanjing, Jiangsu 210016, PR China.
[1] These authors contributed equally to this work.
[*]E-mail: ldshen@nuaa.edu.cn

In the following paper, Cu-Ni multilayer films were prepared by rotating jet electrodeposition (RJE). The Cu plating solution and the Ni plating solution were sprayed alternately during deposition to the rotating cathode surface through the corresponding nozzle. The cross-sectional morphology, microstructure, microhardness, and wear resistance of multilayer films were measured by scanning electron microscope, X-ray diffractometer, microhardness tester, and depth of field microscope, respectively. The results revealed that this novel method had no limit to the technological conditions and avoided the oxidation of the films which existed within the preparation of multilayer films by conventional electrodeposition. The sublayer boundaries of the obtained multilayer films were clear. A semi-coherent interface was formed between the sublayers. The resulting special structure reinforced the properties of the films. The microhardness of the multilayer films increased as the modulation period decreased. When the modulation period was reduced to less than 100 nm, the hardness increased dramatically. In addition, the wear resistance of multilayer films was improved when the modulation period decreased.

Keywords: jet electrodeposition; multilayer films; modulation period; microhardness; wear resistance

1. INTRODUCTION

Multilayer films are formed when different materials are alternately deposited. When the modulation period (the thickness of the film formed during an alternating period) reaches the nanometer scale, nano-multilayer film is formed which has become a top materials research topic [1-4]. The methods that are commonly used when preparing multilayer films include physical, chemical, and electrodeposition methods, and the prepared multilayer films have been extensively used as protective or functional films [5-7]. However, the physical method is costly and the process is complex.

The chemical method is usually performed at high temperatures, which results in poor film quality [8-10]. The electrodeposition method has been favored by researchers for its advantages such as low cost, simple process, and controllable component. In electrodeposition, the single bath method restricts the composition of the plating solution and the deposition potential of each component [11]. The oxidation and dissolution of the film occurs easily during the preparation of the multilayer film when using the dual bath method, and the deposition efficiency is low [12-13]. Therefore, the preparation of multilayer film by electrodeposition has remained within the laboratory stage.

The following paper proposes a novel method that uses rotating jet electrodeposition (RJE) to prepare Cu-Ni nano-multilayer films while avoiding the restrictions in the technological conditions and the oxidation of the films. Moreover, this method retained the original advantages of electrodeposition. In the following experiment, the deposition tank was divided into six independent sections. This got rid of the restrictions in the process conditions and effectively avoided the occurrence of co-deposition. The designed multicomponent rotating device has been used to quantify the continuous alternate deposition between the different plating solutions, thereby preventing the oxidation of the film during the alternating process. When compared with conventional electrodeposition [14-15], the cyclic flow of the plating solution results in the ability to adopt a higher current density, which improved the deposition efficiency. This paper investigated the microstructure and properties of the Cu-Ni multilayer films prepared by RJE.

2. EXPERIMENTAL

The experimental platform that was designed for rotating jet electrodeposition is depicted in Figure 1. The deposition tank was divided into six sections, including two deposition sections, two washing sections, and two abrasive sections. The left was the Ni deposition section and the right was the Cu deposition section. To avoid cross contamination of the plating solution, the lower left and upper right are used as washing sections that cleaned the cathode. The upper left and lower right were abrasive sections filled with ceramic particles (Φ 4~8 mm) that eliminated abnormal bulges on the cathode surface during deposition and reduced film defects [16-17]. A cylindrical stainless steel (Φ 50 mm × 60 mm) was mounted on a rotating shaft to act as a cathode. The substrate surface was pretreated before the experiment by sanding, polishing, degreasing, cleaning, and pickling activation. The Ni plating solution and the Cu plating solution were sprayed alternately onto the cathode surface through the nozzles. The two nozzles were respectively filled with Ni beads and Cu beads which served as anodes. The alternating deposition of Ni ions and Cu ions was achieved by controlling the turn-on and turn-off of the electric current of the specific deposition sections. Since jet electrodeposition was locally deposited [18], the sections did not interact with each other.

The multilayer films with different modulation periods were obtained by varying the switching ratio (the number of cathode rotations when a layer of Cu was formed in an alternating period / the number of cathode rotations when a layer of Ni was formed in an alternating period). The process parameters are shown in Table 1. The Cu plating solution was composed of 220 g/L of $CuSO_4 \cdot 5H_2O$ and 70 g/L of H_2SO_4, and the bath temperature was maintained at 30 °C. The Ni plating solution was comprised of 280 g/L of $NiSO_4 \cdot 6H_2O$, 40 g/L of $NiCl_2 \cdot 6H_2O$, 38 g/L of H_3BO_4, and 2 g/L of

Saccharin, and the bath temperature was kept at 50 °C. The morphology, microstructure, microhardness, and wear resistance of the multilayer films were characterized by the testing equipment shown in Table 2.
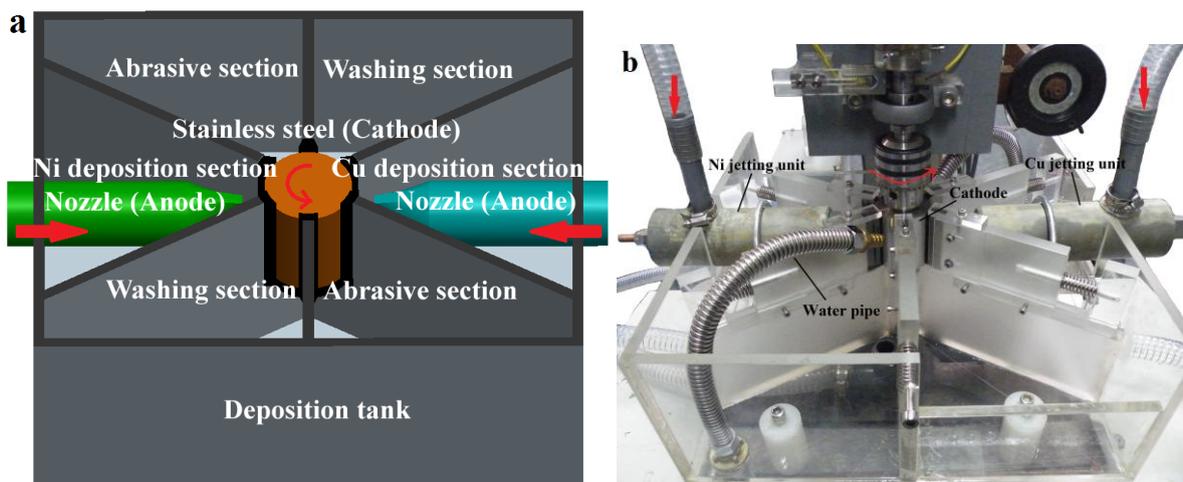
Figure 1. Experimental Platform: (a) Schematic diagram, (b) Physical picture

Table 1. Process parameters

| Parameter	Value
Rate of jet-flow/(mm/s)	3.5
Speed of cathode rotation/(r/min)	8
Distance of anode-cathode/mm	2
Current density of Cu deposition/(A/dm^2)	100
Current density of Ni deposition/(A/dm^2)	80
Switching ratio/(η_{Cu}/η_{Ni})	1/1, 3/3, 5/5, 10/10, 30/30, 50/50, 100/100

Table 2. Test equipments

Instrument (Type)	Manufacturer	Parameter	Characterization
Scanning electron microscope (JSM-7100F)	JEOL Ltd., Japan	-	Cross-sectional morphology
X-ray diffractometer (D/max-2500/PC)	Rigaku Corp., Tokyo, Japan	CuK$_a$, 0.15406 nm, 50 kV, 200 mA, 0.02°, 10°/min	Microstructure
Transmission electron microscope (Tecnai G2)	FEI company	-	
Microhardness tester (HXS-1000A)	Bsida Instruments Co., Chengdu	50 g, 10 s	Microhardness
Depth of field microscope (VHX-600E)	Keyence Co., Ltd., Japan	-	Wear resistance

3. RESULTS AND DISCUSSION

### 3.1. Cross-sectional morphology

The cross-sectional micrographs of the multilayer films obtained at various switching ratios are shown in Figure 2. The dark banded layer was the Cu layer, and the bright banded layer was the Ni layer. Although Wang obtained similar morphologies, the modulation period of the multilayer films he prepared were not within the nanoscale level [19]. As the cathode rotation speed was constant, the number of cathode rotations were proportional to the deposition time. With the reduction of sublayer deposition time, the thickness of the Cu and Ni sublayers decreases gradually. Besides, the boundaries between the different sublayers were relatively clear. The modulation period of the obtained film was reduced from several hundred nanometers to tens of nanometers. According to Faraday's law, the amount of material precipitated on the electrode is proportional to the amount of electricity passed [20]. Therefore, shortening the sublayer deposition time could reduce the sublayer thickness. When the sublayer deposition time was too brief or too long (Fig. 2a, d), the uniformity of the sublayer thickness became poor. The sublayer was too thin when the deposition time was too brief. At this point, the surface roughness of the film had a greater influence on the sublayer thickness. The "tip effect" caused the deposition rate of the metal ions on the convex sections of the film surface to be higher than the concave sections, which led to the difference of the sublayer thickness at the different sites [21]. Excessive deposition time resulted in serious accumulation of film defects. As a result, the surface roughness continually increased, which increased the inhomogeneity of the sublayer thickness.
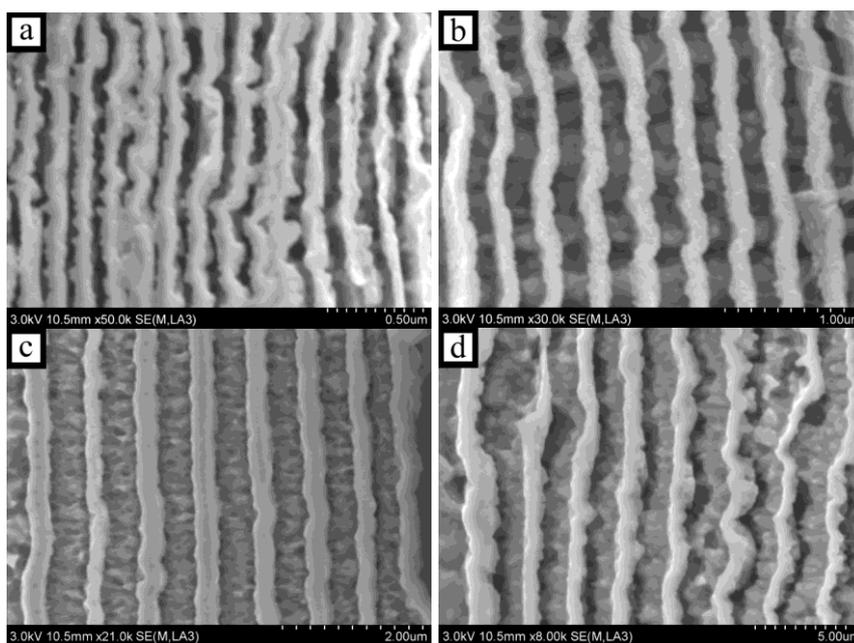
Figure 2. Cross-sectional micrographs of the multilayer films prepared at different switching ratios: (a) 10/10, (b) 30/30, (c) 50/50, (d) 100/100
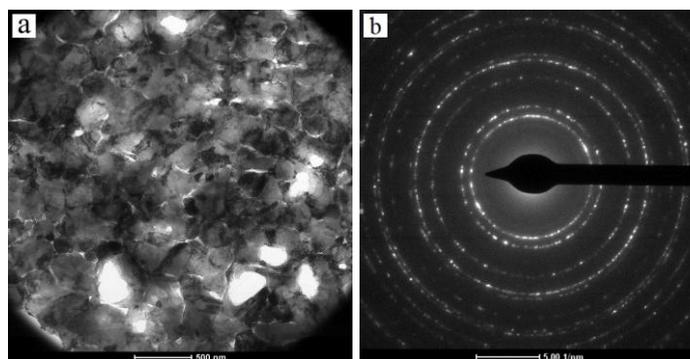
3.2. Microstructure

The X-ray diffraction patterns of the nano-multilayer films obtained at various switching ratios are shown in Figure 3. The corresponding crystal planes of the three diffraction peaks were (111), (200), and (220). Preferential orientation was found on the (111) crystal surface of the film. It is known that the (111) crystal surface has high atomic density and low surface energy in the face-centered cubic structure, which was beneficial in improving the wear resistance of the film. When there was a long sublayer deposition time, the diffraction patterns of the multilayer films exhibited double peaks due to the existence of the Cu and Ni layers with different lattice constants. It has been reported previously that Barshilia prepared Cu/Ni multilayer films by magnetron sputtering, and the diffraction patterns of the resulting films showed similar peaks [22]. Such double peaks were also observed when Yan deposited multilayer films by electron beam evaporation [23]. As the sublayer deposition time shortened, the double peaks of the multilayer film began to become single peaks, and the intensity of the diffraction peaks for each crystal surface was greatly enhanced. The dashed and dotted lines indicated the positions of the standard X-ray diffraction peaks of Cu and Ni. A comparison showed that the diffraction peaks of the multilayer films that had various switching ratios shifted by different degrees. A further analysis of the X-ray diffraction patterns showed that there were small amounts of Cu-Ni alloy in the multilayer film. Because the atomic radii of Cu and Ni differ little, their alloys formed substitutional solid solutions. This resulted in their diffraction peaks of the films being shifted [24]. Moreover, the modulation period of the film reached the nanometer scale when the sublayer deposition time was short. There was nano-interface effect between the sublayers of Cu and Ni at this point, which caused the diffraction peaks to shift [25].
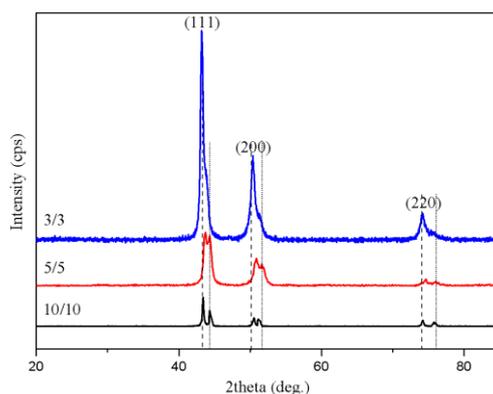

Figure 3. X-ray diffraction patterns of the multilayer films prepared at different switching ratios

The TEM field diagram of Cu-Ni multilayer film and its corresponding electron diffraction pattern as the switching ration was 10/10 are depicted in Figure 4. The structure of multilayer films was quite different from that of monolayer films [26]. The crystal growth mode of the films changed fundamentally during the deposition. A possible change was the gradual transition from island growth to layered growth. The X-ray diffraction patterns and the diffraction rings obtained here showed that the Cu and Ni were mixed and fused at the interface. The differences between the lattice constants of Cu and Ni was small (the lattice constant of Cu was 361.5 pm and the lattice constant of Ni was 352.4 pm), which resulted in the epitaxial growth of the multilayer films at the interface to form the

superlattice structures [27]. These mixing and fusions could be understood as the special structure of Cu-Ni multilayer films. The actual structure of the Cu-Ni multilayer films that were prepared in this paper is shown in Figure 5, forming the three layer structure of Cu/CuNi/Ni. In fact, there was no obvious dividing line between the Cu-Ni alloy layer, the Cu layer, and the Ni layer, but the boundaries were set artificially due to the different molecular structures. The superlattice structure of the film was referred to as the semi-coherent interface because the pure Cu layer and the pure Ni layer were in the multilayer film [28]. The only time a full coherent interface could be formed is when the modulation period was below a critical value (< 10 nm) [29].

Figure 4. TEM field diagram of Cu-Ni multilayer film (a) and its corresponding electron diffraction pattern (b)
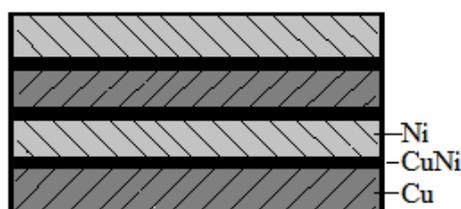

Figure 5. Schematic diagram of the three layer structure of Cu-Ni multilayer film

3.3. Microhardness

The microhardness of the multilayer films obtained at various switching ratios are shown in Figure 6. As the sublayer deposition time decreased, the microhardness of the multilayer films gradually increased. In other words, the narrower the modulation period, the higher the microhardness. Furthermore, the microhardness of the resulting film rose faster when the number of cathode rotations were less than 10. It could be deduced that when the switching ratio was 10/10 (the number of cathode rotations were 10), the modulation period of the obtained multilayer film was about 120 nm (Fig. 2a). Therefore, it was concluded that the microhardness of the film with the modulation period in the nanoscale was much higher than that of the film with the modulation period in the submicron scale. In previous studies, Zhang deposited Cu-Ni multilayer films by ion-assisted magnetron sputtering in order to study the microhardness. It was found that the microhardness of the film with a modulation

period of 20 nm was much larger than that of the film with a modulation period of several hundred nanometers [30], which was consistent with the above conclusions.
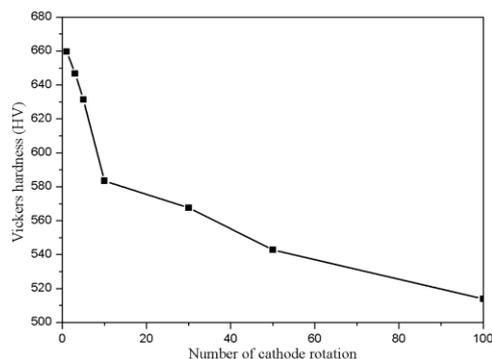

Figure 6. Microhardness of Cu-Ni multilayer films

The substantial enhancement of hardness was primarily attributed to the nanometer size effect of nano-multilayer film. The presence of the semi-coherent interface in the film acted as a barrier to make glide dislocations difficult to cross the interface, and consequently played a dominant role in strengthening the film properties. Although the microhardness of the film varied with the modulation period, the overall variation trend was obviously consistent with the Hall-Petch relationship [31]. As the modulation period of the multilayer film was reduced further, the hardness continued to increase, but it gradually deviated from the strength of the epitaxy based on the Hall-Petch equation. Such variation trend was also observed in the preparation of Cu/Ni multilayer films by Fu [32]. If the modulation period continued to decrease, the structure of nano-multilayer film would evolve from a semi-coherent interface to a full coherent interface and the hardness would decrease due to the decrease of the thickness of coherent interface [33].

3.4. Wear resistance

The worn surface morphologies of the nano-multilayer films obtained at various switching ratios are shown in Figure 7. When the modulation period was thin (Fig. 7a), the worn surface of the film showed a slight wear mark and the wear form was dominated by micro wear. While the scratches were visible on the worn surface as the modulation period increased and the wear form gradually changed to abrasive wear (Fig. 7b, c). The width and depth of the surface scratches increased as the modulation period continued to increase (Fig. 7d), where a small number of adhesive blocks were observed. The wear form was chiefly abrasive wear at this point, but was accompanied by a small amount of adhesive wear. The width and depth of surface scratches of the Cu-Ni nano-multilayer films with various switching ratios are shown in Table 3. With the decrease of sublayer deposition time, the width and depth of surface scratches decreased. Thus, the wear resistance of nano-multilayer films was obviously improved when the modulation period was reduced. Martínez prepared CrN/Cr multilayer films by magnetron sputtering and evaluated their tribological behavior. The results showed that the

wear rate of multilayer films was much smaller than that of CrN and Cr monolayer films, and decreased with the decrease of modulation period [34].
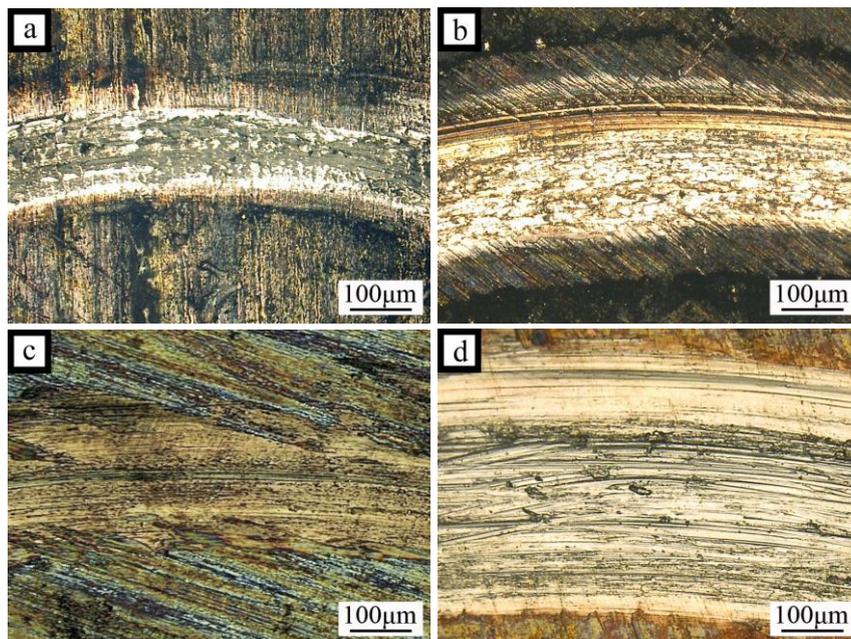
Figure 7. Worn surface morphologies of the multilayer films prepared at different switching ratios: (a) 1/1, (b) 3/3, (c) 5/5, (d) 10/10

Table 3. Width and depth of surface scratches of the multilayer films with different switching ratios

Switching ratio/(η_{Cu}/η_{Ni})	Width (μm)	Depth (μm)
1/1	145.5	4.4
3/3	267.1	6.9
5/5	259.9	11.1
10/10	489.2	20.7

Wear resistance improvement was largely caused by the semi-coherent interface in the Cu-Ni multilayer films. There were a large number of internal interfaces parallel to the substrate in the multilayer films, which could split and skew the cracks, thereby preventing crack propagation and providing dislocation resistance. The failure test showed that its extension direction changed when the crack reached the interface, thus effectively preventing the penetration of the crack and avoiding the failure of the entire film [35]. Cao has found that the interaction between dislocations and interfaces plays a crucial role in the plastic deformation during indentation on Ni/Al multilayer films, and the friction coefficient of the multilayer film is smaller than that of the pure Ni thin film [36]. In addition, the hardness was an important factor affecting the wear resistance of multilayer films. As discussed above, the microhardness of multilayer film increased as the modulation period decreased, thereby resulting in an increase of wear resistance.

4. CONCLUSION

RJE had no restrictions to the technological conditions and effectively avoided the oxidation of the films in alternating deposition. As a result, the sublayer boundaries of the resulting multilayer film were clear and the sublayer thickness was relatively uniform.

The semi-coherent interface was formed between the Cu layer and the Ni layer, which was confirmed by analyzing the microstructure of the multilayer film. The actual structure of the multilayer film was Cu/CuNi/Ni. The special structure enhanced the interface effect of the nano-multilayer films and became the primary source that strengthened the performance of the film.

The microhardness of multilayer films was enhanced as the modulation period decreased. Moreover, the hardness of the nanoscale modulation period film was much higher than the submicron scale modulation period film. By reducing the modulation period, the wear resistance of the film was improved. The form of wear changed from slight wear to abrasive wear, even to adhesive wear.

References

1. B. J. Liu, B. Deng, Y. Tao, *Surf. Coat. Technol.*, 240 (2014) 405.
2. P. L. Sun, C. H. Hsu, S. H. Liu, *Thin Solid Films,* 518 (2010) 7519.
3. S. H. Yao, Y. L. Su, W. H. Kao and T. H. Liu, *Tribol. Int.*, 39 (2006) 332.
4. P. L. Sun, C. Y. Su, T. P. Liou, *J. Alloys Compd.*, 509 (2011) 3197.
5. M. Pătru, C. Gabor, D. Cristea, *Surf. Coat. Technol.*, 320 (2017) 284.
6. S. J. Yan, T. C. Fu, R. Y. Wang, *Nucl. Instrum. Methods Phys. Res. B*, 307 (2013) 143.
7. K. E. Bae, K. W. Chae, J. K. Park, *Surf. Coat. Technol.*, 276 (2015) 55.
8. C. X. Zhang, C. G. Zhou, H. Peng, *Surf. Coat. Technol.*, 201 (2007) 6340.
9. H. K. Moon, J. Yoon, H. Kim and N. E. Lee, *Met. Mater. Int.*, 19 (2013) 611.
10. N. Sun, C. J. Li, Y. T. Fu, *Superlattices Microstruct.*, 97 (2016) 313.
11. V. Thangaraj, N. Eliaz, A. C. Hegde, *J. Appl. Electrochem.*, 39 (2009) 339.
12. N. Maleak, P. Potpattanapol, N. N. Bao, *J. Magn. Magn. Mater.*, 354 (2014) 262.
13. P. Pascariu, S. I. Tanase, D. P. Tanase, *Mater. Chem. Phys.*, 131 (2012) 561.
14. H. J. Zheng, F. Q. Tang, M. Lim, J. Power Sources, 193 (2009) 930.
15. B. G. Tóth, L. Péter and I. Bakonyi, J. Electrochem. Soc., 158 (2011) D671.
16. D. Z. Huang, L. D. Shen, J. S. Chen, *Trans. Indian. Inst. Met.*, 67(3) (2014) 351.
17. G. F. Wang, Z. J. Tian, Z. D. Liu, *Int. J. Electrochem. Sci.*, 10 (2015) 6844.
18. M. S. Rajput, P. M. Pandey, S. Jha, *J. Manuf. Process.*, 17 (2015) 98.
19. G. F. Wang, L. D. Shen, L. M. Dou, *Int. J. Electrochem. Sci.*, 9 (2014) 220.
20. H. Lee, W. Lee, J. Y. Kim, *Electrochim. Acta*, 87 (2013) 450.
21. X. Liu, L. D. Shen, M. B. Qiu, *Surf. Coat. Technol.*, 305 (2016) 231.
22. H. C. Barshilia, K. S. Rajam, *Surf. Coat. Technol.*, 155 (2002) 195.
23. X. L. Yan, E. Coetsee, J. Y. Wang, *Appl. Surf. Sci.*, 411 (2017) 73.
24. D. J. Qiu, H. Z. Wu, A. M. Feng, *Appl. Surf. Sci.*, 222 (2004) 263.
25. D. Mott, J. Galkowski, L. Y. Wang, *Langmuir,* 23 (2007) 5740.

26. G. L. Zhao, Y. Zou, Y. L. Hao, *Arch. Metall. Mater.*, 60 (2015) 1003.
27. X. Y. Zhu, X. J. Liu, R. L. Zong, *Mater. Sci. Eng*. A, 527 (2010) 1243.
28. S. Y. Weng, H. M. Ning, N. Hu, *Mater. Des.*, 111 (2016) 1.
29. A. Misra, J. P. Hirth, H. Kung, *Philos. Mag. A*, 82 (2002) 2935.
30. X. H. Zhang, D. X. Liu, G. H. Liu, *Tribol. Int.*, 44 (2011) 1488.
31. J. Man, S. Zhang, J. F. Li, *Surf. Coat. Technol.*, 249 (2014) 118.
32. T. Fu, X. H. Peng, X. Chen, *Sci. Rep.*, 155 (2016) 1.
33. Y. C. Qian, J. Tan, Q. Q. Liu, *Surf. Coat. Technol.*, 205 (2011) 3909.
34. E. Martınez, J. Romero, A. Lousa, *Surf. Coat. Technol.*, 163 (2003) 571.
35. H. Holleck, M. Lahres, P. Woll, *Surf. Coat. Technol.*, 41 (1990) 179.
36. Y. Z. Cao, J. J. Zhang, Y. C. Liang, *Appl. Surf. Sci.*, 257 (2010) 847.